Chapter I

INTRODUCTION

Recently, nano-technology has attracted considerable scientific interest due to the new potential uses of nano-materials (NMs) with particle size in nanometer (10^{-9}m) scale [1]. The nano-particles (NPs) show unique physico-chemical properties different from those of the conventional materials [2]. Indeed, NMs can change the concrete world, due to their properties at ultra-fine level. Thus, various industries may be able to re-engineer many existing products and to design new as well as novel products that function at unprecedented levels**.** There is a great interest in replacing nano materials in concrete structure that improve the physico-mechanical properties of concrete [3].

Nanotechnology has changed our vision, expectations and abilities to control the material world. The developments in nano-science can also have a great impact on the field of construction materials and other fields in science (physics, chemistry, bioscience, etc.) [4].

Nano-technology is one of the most active research areas with both novel science and useful applications that has gradually established in the last two decades. It is the creation of materials and devices by controlling of matter at the level of atoms, molecules and super molecular (nano-scale) structure. Better understanding and engineering of cement based materials at the nano-level will definitely result in a new generation of concrete, stronger, more durable and possibly, with the whole range of newly introduced ‘‘smart’’ properties [5].

Nano-particles are among prospective materials in the field of civil engineering which have ahigh-surface area for providing high chemical reactivity [6]. They act as nucleation centers, contributing to the development of the hydration of OPC paste. However, due to the high surface area very strong attractive properties can be obtained.

Some researchers have employed nano-particles into cementitious materials based on Portland cement (OPC) to modify some properties of this system. Regarding the addition of nano-particles to OPC paste, they have important implications for the hydration and the microstructure of the paste such as an increase in the initial hydration rate, as in the amount of CSH gel of the paste through pozzolanic reaction, porosity reduction, and improvement of mechanical properties of the CSH gel itself (greater alumina-content, longer silicate chains) [7]. Therefore, the formation of nano-particles of the hydration products (C–S–H, calcium hydroxide, ettringite, monosulfate, unhydrated particles and air voids), to overcome durability

issues, is a crucial step in the concrete eco-efficiency [8].To date, nanotechnology applications and advances in the construction as well as building materials fields have been uneven [9].

Nano-Fe_2O_3 has important advantages for the hydration and microstructure of cement paste to increase the rate of hydration and the amount of formed CSH gel [10,11]. OPC admixed with 1% NF gives the optimum content to achieve fire resistance than 2 and 3% NF. It shows higher compressive strength as well as bulk density and lower total porosity. The bulk density and total porosity of cement pastes decrease with heat treatment up to nearly 250 ^{o}C then increase, whereas the compressive strength increases up to 450 ^{o}C then decreases with heat treatment up to 600 ^{o}C.

Chapter II

LITERATURE REVIEW

Nanotechnology is based on synthesizing nano-particles with specified characteristics to be used in different applications related to the industry, medicine, agriculture, etc. A nano-particle is a microscopic particle whose size is measured in nano-meters (nm). It is defined as a particle with at least one dimension less than 200-nm. During the last ten years, not only the nano-products were utilized to improve the quality and durability of products, but also new approaches were developed to handle traditional problems.

Nanotechnology helps in producing materials with prospective properties, for each field of science (physics, chemistry, bio-science as well as construction materials). Nanoparticles belong to the materials in the field of civil engineering which have a high surface area to provide high chemical reactivity. Some researchers have employed nanoparticles into cementitious materials based on ordinary Portland cement to modify the properties of this system. They have important advantages for the hydration and microstructure of cement paste to increase the rate of hydration and the amount of formed CSH gel.

There are many advantages including low environmental impact, high strength and light weight structures with low CO_2 emissions, also enhance mechanical property, vibration damping capacity, air void content, low permeability, steel rebar corrosion resistance, and workability as well as alkali-silica mitigations, where the beneficial action of the nanoparticles on the microstructure and performance of cement-based materials can be explained by the following factors [12]:

1. Nanoparticles fill the voids between cement grains, resulting in the immobilization of free water (filler effect).
2. Well-dispersed nanoparticles act as centers of crystallization of cement hydrates, hence accelerating the hydration.
3. Nanoparticles favor the formation of small-sized crystals (such as $Ca(OH)_2$, AFm) and small-sized uniform clusters of C–S–H.
4. Nanoparticles accelerate the pozzolanic reactions, resulting in the consumption of $Ca(OH)_2$ and formation of an additional C–S–H gel.

5. Nanoparticles improve the structure of the aggregates interfacial zone, resulting in a better bond between aggregates and cement paste.
6. Nanoparticles provide crack arrest and interlocking effects between the slip planes, which improve the toughness, shear, tensile and flexural strength of cement-based materials.

Ali Nazari, (2011) [13] investigated the effect of with partial replacement of cement with Fe_2O_3 nano-particles on water absorption, velocity of water absorption, coefficient of water absorption, workability, and setting time of binary blended concrete. The results showed that using Fe_2O_3 nano-particles up to maximum replacement of 2.0% produces concrete with improved resistant to water permeability. Fe_2O_3 nano-particles can improve the filler effect and also the high pozzolanic action of fine particles increases substantially the quantity of C—F—H gel. If this phenomenon joints with low water-to-cement ratio, it can improve the microstructure in the interfacial transition zones and thus the value of C—F—H gel results in decreasing the water permeability. The results also show that the workability and setting time of fresh concrete were decreased by increasing the content of Fe_2O_3 nano-particles [13]. Compressive, flexural and split tensile strength together with coefficient of water absorption of high performance self-compacting concrete containing different amount of Fe_2O_3 nano-particles have been investigated. The strength and the water permeability of the specimens have been improved by adding Fe_2O_3 nano-particles in the cement paste up to 4.0 wt%. Fe_2O_3 nano-particle as a foreign nucleation site could accelerate C-S-H gel formation as a result of increased crystalline $Ca(OH)_2$ amount especially at the early age of hydration and hence increase the strength of the specimens. In addition, Fe_2O_3 nano-particles are able to act as nano-fillers and recover the pore structure of the specimens by decreasing harmful pores to improve the water permeability. Several empirical relations have been presented to predict the flexural and the split tensile strength of the specimens by means of the corresponding compressive strength at a certain age of curing. Accelerated peak appearance in conduction calorimetry tests, more weight loss in thermogravimetric analysis and more rapid appearance of peaks related to hydrated products in X-ray diffraction results indicate that Fe_2O_3 nanoparticles up to 4 wt% could improve the mechanical and the physical properties of the specimens [14].

Chapter III

MATERIALS AND EXPERIMENTAL TECHNIQUE

1. Materials

The materials used in this investigation are Ordinary Portland cement (OPC) provided from Yamama cement Company, Riyadh, KSA. The chemical and mineralogical composition of OPC is given in Table (1). Basic ferric acetate [$Fe(CH_3COO)_2OH$] as chemical grade.

Table 1: Chemical composition and phase composition OPC

Oxides, %	OPC
SiO_2	20.32
Al_2O_3	4.34
Fe_2O_3	4.30
CaO	64.58
MgO	0.75
SO_3	2.12
K_2O	0.06
Na_2O	0.12
TiO_2	–
P_2O_5	–
L.O.I	2.52
Insoluble residue	0.56

The NF was prepared by thermal decomposition of basic ferric acetate which heated in a muffle furnace at 300 and 500 ^oC with heating rate 10 ^oC/min for one hour soaking time. The thermal behavior of basic ferric acetate during heating under nitrogen atmosphere at rate of ^oC/min was carried out by using thermal analyzer. Figure 1 show the thermal gravimetric (TGA) thermogram of ferric acetate heated up to 700 ^oC.

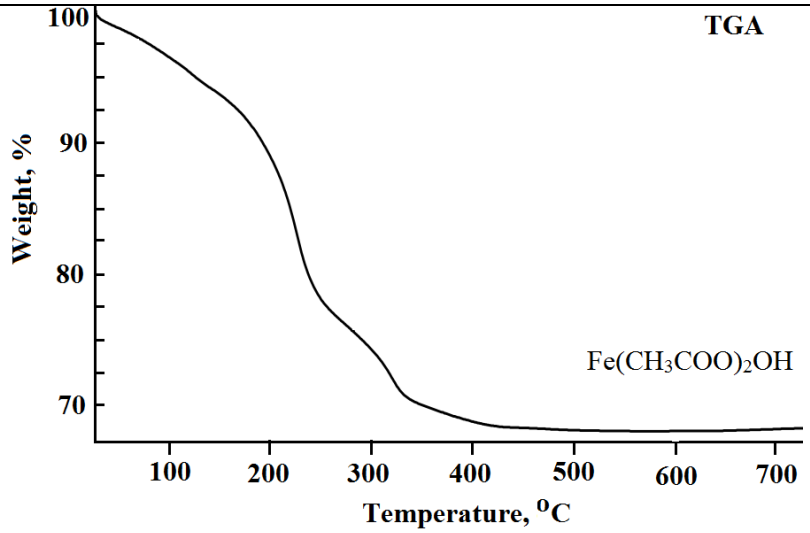

Figure 1: TGA thermogram of ferric acetate

Figure 1 illustrates the (TG) analysis of the basic ferric acetate up to 700o C. It gives TGA loss 23.89%, up to 300 ^{o}C. This mainly due to the loss associated with desorption of acetone and carbon dioxide from ferric acetate with the formation of hematite [15]. At 700 oC, the total loss is 32.08%. The observed difference between the TGA loss at 300 and 700oC is due to the formation of magnetite Fe_3O_4, which is accompanied by release of oxygen.

TEM shows the crystal size of NF prepared at 300 ^{o}C is 10.5 nm as shown in Figure 2. Figure 3 shows the formation of hematite and magnetite as the main phase. The presence of magnetite in the fired product at is mainly due to the insufficient atmospheric air to oxidize the magnetite Fe_3O_4 to hematite Fe_2O_3.

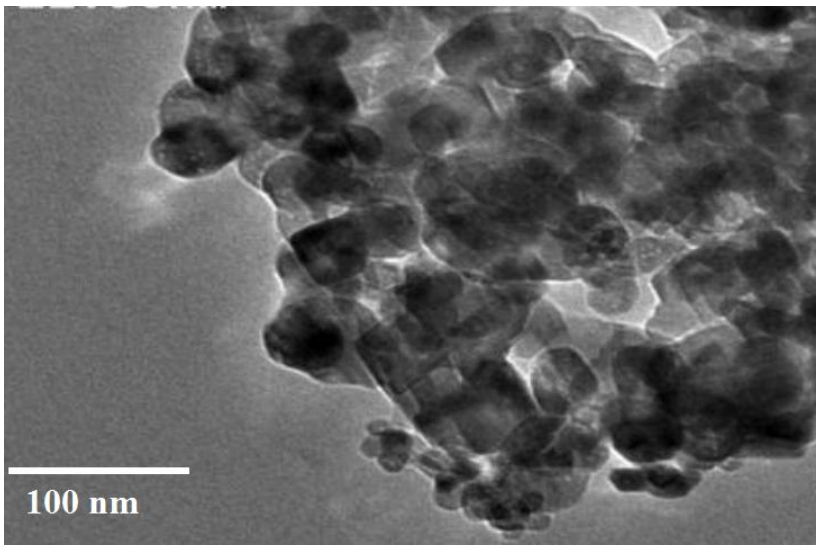

Figure 2: TEM of NF fired at 300 ^{o}C

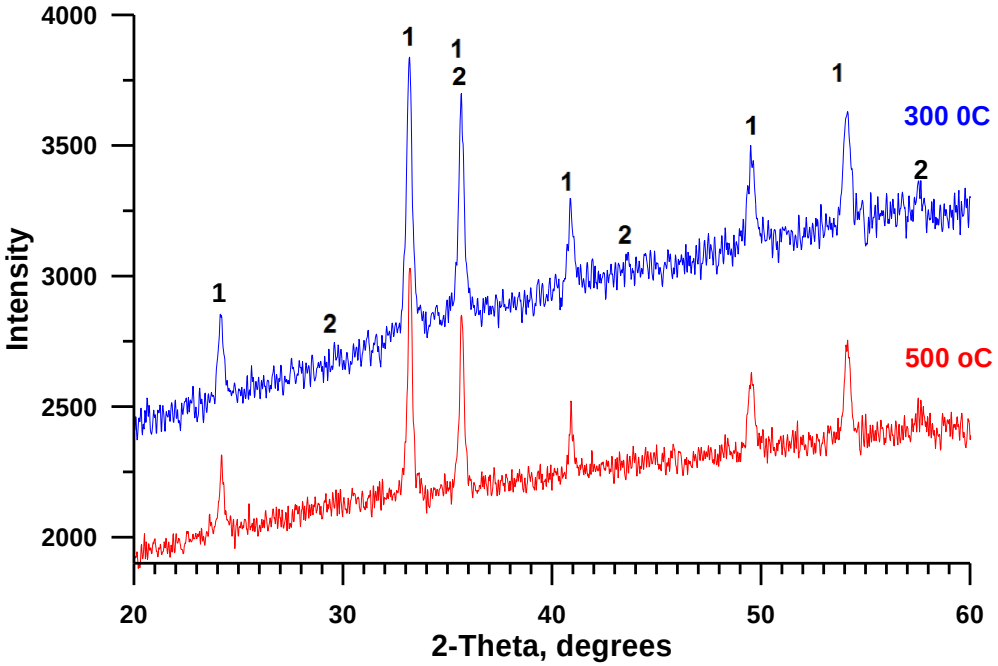

Figure 3: XRD of NF fired at 300 and 500 ^{o}C for one hour; 1= Fe_2O_3, 2= Fe_3O_4

2. Preparation of cement pastes:

Mixes were prepared by substitution of OPC with 0, 1 and 2 mass% NF prepared at 300 and 500 ^{o}C. The dry constituents of each mix were mechanically mixed for one hour in a porcelain ball mill using four balls to attain complete homogeneity then kept in air tight containers.

The mixing of cement powder was carried out with water/cement ratio = 0.3. The admixed cement was placed on non-absorbent surface and a crater was formed in the center. The mixing operation was then completed by continuous vigorous mixing for three minutes with gauging trowel. At the end of mixing, the pastes were directly poured in 2cm cubic stainless steel moulds into two approximately equal layers. Each layer was compacted and pressed until homogenous specimen was obtained then manually vibrated for a few minutes to remove any air bubbles to give a better compaction of the paste. Immediately after molding, the moulds were cured in a humidity chamber at 100% RH at room temperature (22 ^{o}C) for the first 24 hours, then demoulded and cured under tap water till time of testing. The cylindrical specimens prepared shown in Figure 4.

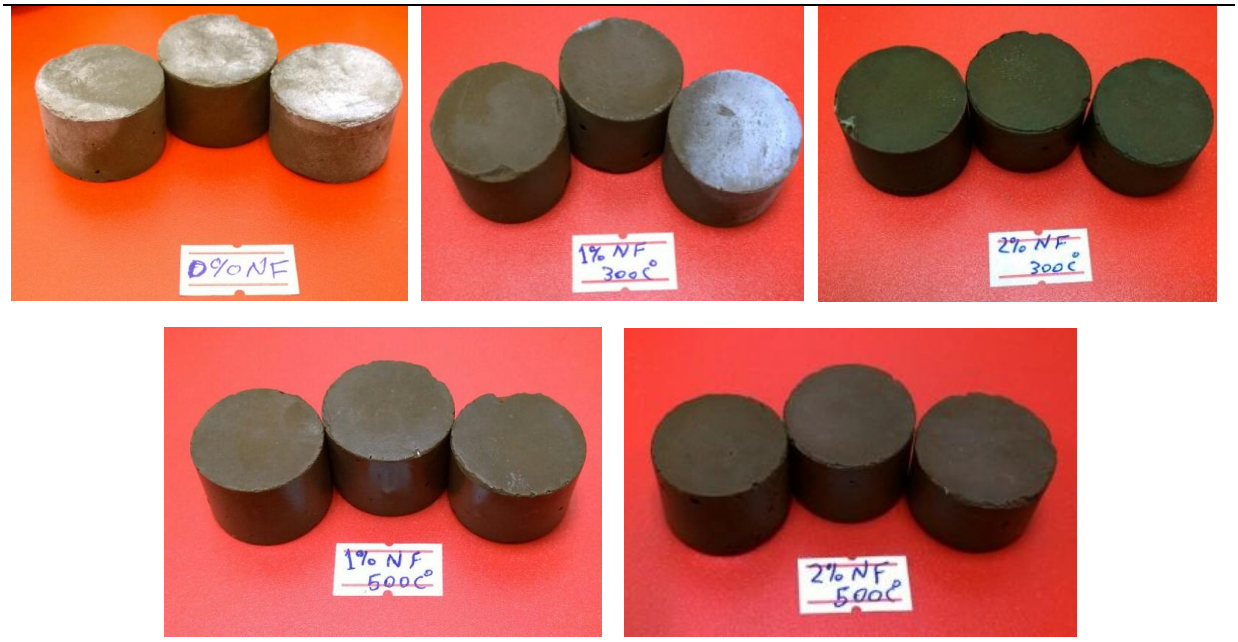

Figure 4: Specimens prepared

3. Methods of investigation

3.1. Determination of compressive strength

Three cubes were used for the compressive strength determination of cement paste (ASTM Designation: C-150, 2007). The compressive strength was done on a compression machine with maximum capacity of 600 KN force as shown in Figure 5. The compressive strength was carried out on three samples as described by ASTM Specifications [16].

Figure 5: The compression machine.

3.2. Determination of chemically combined water contents:

The chemically combined water contents (W_n), was determined in a similar manner to (W_t). It is the weight loss of the dried paste on ignition at 900^{o}C. Two representative samples of the dried specimen about 2 g, each were exactly weighed in a porcelain crucibles and ignited for one hour at 1000^{o}C in a muffle, cooled in a desiccator, then weighed [17]. The combined water content was calculated as W_n using the following equation:

$$W_n = \left[\frac{(W_1 - W_2)}{W_2}\right] - [L + A]$$

where**:**

W_n is the non-evaporatable water,

W_1 is the weight of sample before ignition,

W_2 is the ignited weight of specimen,

L is the ignition loss of unhydrated specimen and

A is the amount of water held by the free lime.

3.3. Determination of free lime contents:

This method is more rapid and applicable for the determination of free CaO, as well as, $Ca(OH)_2$. It is based on the extraction of Ca^{2+} by ethylene glycol method [18]. Free lime present in the sample will react with ethylene glycol forming calcium glycolate. This glycolate was titrated with standard hydrochloric acid:

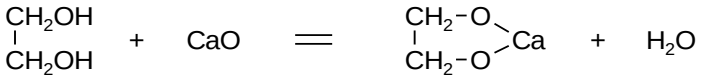

Ethylene glycol Calcium glycolate

then,

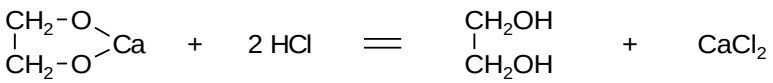

About 0.5 g of the sample is placed in small conical flask with 25 ml of ethylene glycol and a pinch of clean quartz grains. The flask is closed with air reflux and shaken on a water bath at 60-70^{o}C for 1 hour. The sample is filtered through filter paper then washed three times

with about 15 ml glycol. The filtrate is titrated with standardized 0.1 N aqueous HCl by using phenolphthalein as indicator till the pink colour disappeared (end point). The free CaO content of the sample was calculated as:

$$\% \text{ CaO} = \left[\frac{100 \text{ EV}}{\text{w}} \right]$$

where:

E is the equivalence of standard HCl solution in g CaO per ml,

V is the milliliters of HCl solution required by the sample, and

w is the weight of sample taken.

3.4. Phase composition:

The crystalline phases of cement pastes were identified using XRD technique of BRUXER, Axs D8 ADVANCE A8, and GERMANY Diffractometer. The samples were finely ground to pass a 200-mesh sieve. The identification of all samples was confirmed by computer-aided search of the PDF database obtained from the Joint Committee on Powder Diffraction Standards-International Center for Diffraction Data (JCPDA-ICDD), 2001.

Thermal gravimetric analysis (DTA/TGA) was carried out using DTA-50 Thermal Analyzer (Schimadzu Co., Tokyo, Japan). A dried sample of about 50 mg (≈53 μm) was used at heating rate 10 °C/min under nitrogen atmosphere.

The scanning electron microscope (SEM) was investigated with Inspect S (FEI Company, Holland) equipped with an energy dispersive X-ray analyzer (EDX). SEM was used to examine the microstructure of the fractured composites at the accelerating voltage of 200–30 kV and Power zoom magnification up to 300,000×.

Chapter IV

RESULTS AND DISCUSSION

4. 1. Compressive strength:

The effect of NF content on the compressive strength of hydrated cement pastes is given in Table (2) and graphically plotted in Figure 6. The compressive strength increases with curing time for all hydrated cement pastes, this is due to the continuous hydration as well as the formation of successive amounts of calcium silicate hydrates (C-S-H) (the main source of strength) and calcium aluminosilicate (C-A-S-H) hydrates. These hydrated products accumulate in the water filled open pores to form a more compact body [13]. The compressive strength of the cement pastes increases sharply with NF content up to 2 mass% fired at 300 ^{o}C.

Table 2: Compressive strength of cement pastes containing NF

Mix No.	Compressive strength, Kg/cm^2
I	585.96
II	668.58
III	720.51
IV	584.20
VI	609.31

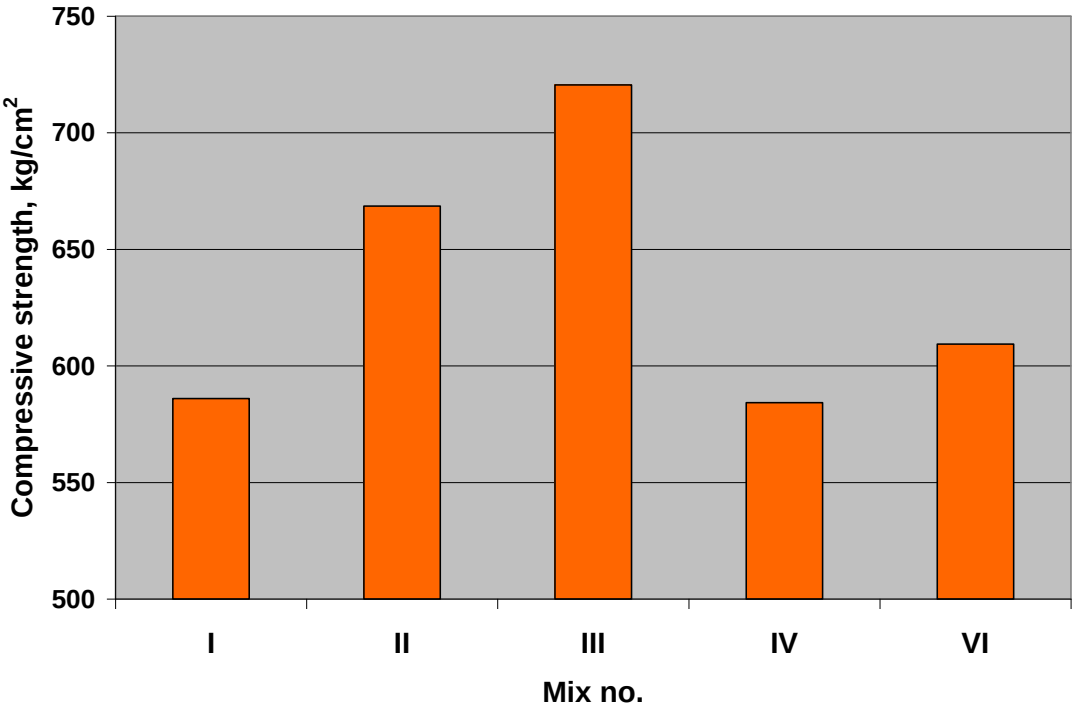

Figure 6: Compressive strength of cement pastes containing NF

NF nano-particles has a higher degree of hydration reaction speed than OPC pastes, because NF nano-particles is characterized by its unique surface effects, smaller particle sizes, and higher surface energy. The improvements of compressive strength in the presence of NF, is due to the fact that, NF behaves not only as a filler to improve nano-structure, but also as an active pozzolana to promote the pozzolanic reaction. Both the nucleation and pozzolanic effects of NF lead to more accumulation and precipitation of hydration products in the open pores originally filled with water, leading to the formation of homogeneous, dense and compact nano-structure. The compressive strength of the cement pastes containing NF fired at 500 ^{o}C, shows a lower values compared with those pastes containing NF fired at 500 ^{o}C.

4. 2. Chemically combined water contents:

The chemically combined water contents of cement pastes hydrated up to 7 days as a function of NF contents are given in Table 3 and graphically represented in Figure 7. It is clear that chemically combined water content increases with curing time for all hydrated cement pastes. This is mainly due to the continuous hydration of cement phases, leading to the formation of more hydrated products, which precipitated in the available open pores system. The values of chemically combined water contents increase with the NF content up to 1mass%. Increase of the content of NF nano-particles up to 2%, the chemically combined water content decreases, but still higher than that of the neat OPC paste as shown in Figure 7.

Table 3: Chemically combined water contents of cement pastes containing NF fired at 300 and 500 ^{o}C

Mix No.	Chemically combined water contents, %
I	19.44
II	21.71
III	21.31
IV	20.00
VI	19.79

The increase in the combined water contents in the presence of different contents of NF nano-particles is mainly due to the higher pozzolanic activity of NF nano-particles. NF nano-particles reacts with the liberated CH during the hydration of cement phases to form additional hydrated products such as C-S-H, C-A-H, and C-A-S-H as well as C—F—H gel. NF nano-particles act as nucleation sites to accelerate the hydration. NF nano-particles accelerates the cement hydration largely in the early age with a reduction in low-stiffness C–S–H gel and an

increase in high-stiffness C–S–H gel **[13,14]**. The enhancement of NF nano-particles is due to the filling of the voids of cement pastes, which leads to a dense and stronge structure.

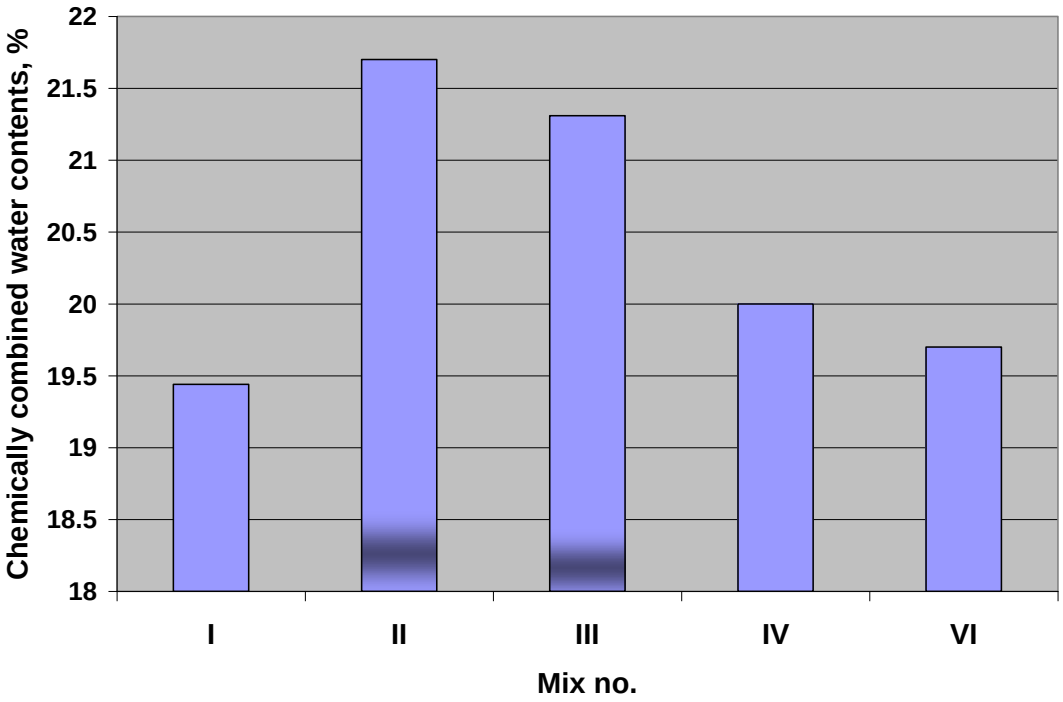

Figure 7: Chemically combined water contents of cement pastes containing NF

4. 3. Free lime contents:

Free lime contents (FL%) of cement pastes with 0, 1, and 2% of NF nano-particles hydrated up to 7 days are given in Table 4. These data are graphically represented in Figure 8. The results show that the free lime content of OPC paste increases with curing ages due to continuous hydration of alite (C_3S) and belite (β-C_2S) phases liberating portlandite (CH) during the hydration reaction [17,19]. On the other side, the free lime contents of all cement pastes containing NF nano-particles shown an decrease due to the formation of C—F—H gel. There are two processes; first is lime production from the hydration of cement phases (C_3S and β-C_2S); second is the lime consuming (pozzolanic reaction). NF accelerates the hydration rate of cement phases (C_3S and β-C_2S). The increasing in the compressive strength is due to the rapid consuming of $Ca(OH)_2$ which was formed during hydration of OPC at early ages related to the high reactivity of NF nano-particles.

Table 4: Free lime contents of cement pastes containing NF fired at 300 and 500 ^{o}C

Mix No.	Free lime contents, %
I	10.592
II	9.1728
III	8.569
IV	10.364
VI	10.274

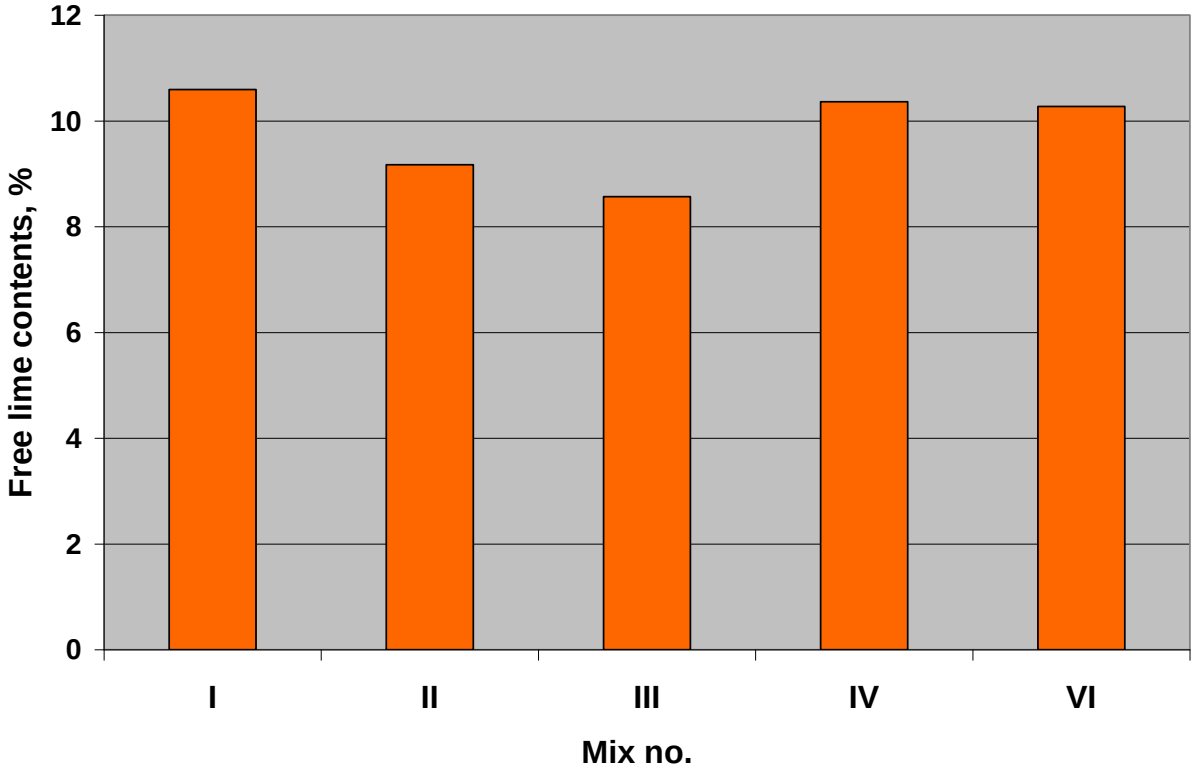

Figure 8: free lime contents of cement pastes containing NF

4. 4. Phase composition:

The phase composition of the formed hydration products was identified using differential thermal analysis (DTA/TGA) and X-ray diffraction (XRD) analysis as well as scanning electron microscopy (SEM).

4. 4. 1. XRD diffraction patterns:

X-ray diffractograms of the hardened I, II, III, IV and VI cement pastes containing NF fired at 300 and 500 ^{o}C are shown in Figure 9,10. Figure 9 shows the X-ray diffraction lines of mixes I, II and III containing 0, 1, and 2% of NF nano-particles hydrated up to 7 days. X-ray diffractograms show the presence of hydrated and anhydrated phases namely, CH, β-C_2S, C_3S, $C\bar{C}$ and CSH. The peak intensity of C-S-H and CH corresponding to 1% of NF nano-particles increases than those containing 0, and 2% of NF nano-particles. Mix II is the optimum mix composition.

Figure 10 shows the X-ray diffraction lines of mixes IV and VI containing 1, and 2% of NF nano-particles fired at 500 ^{o}C. X-ray diffractograms show the presence of hydrated and anhydrated phases namely, CH, β-C_2S, C_3S, $C\bar{C}$ and CSH. The peak intensity of C-S-H and CH corresponding to 2% of NF nano-particles increases than those containing 1% of NF nano-particles.

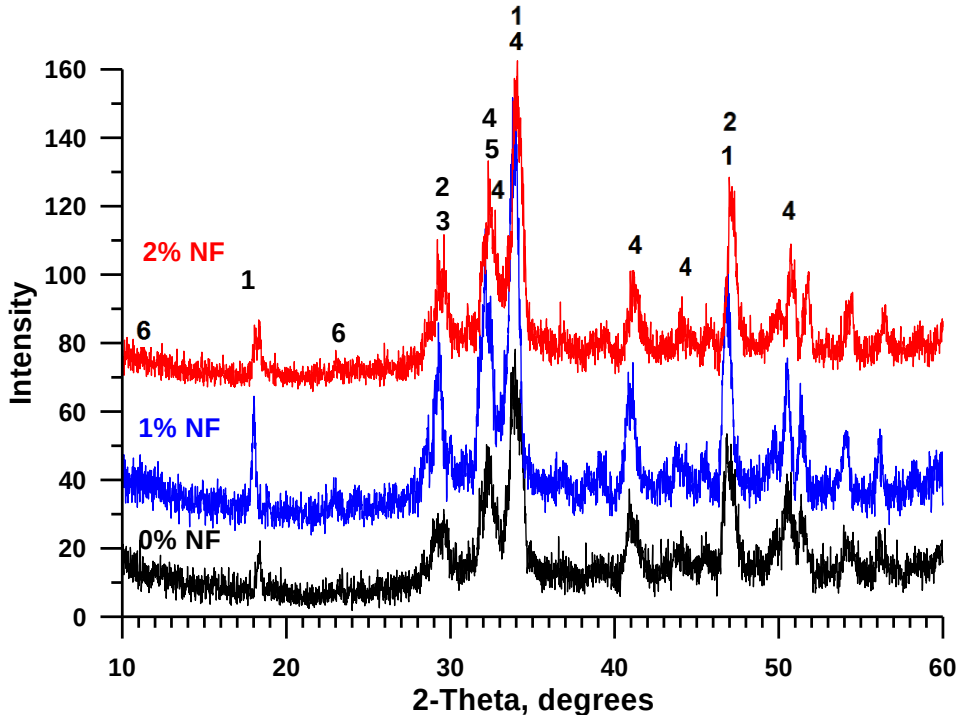

Figure 9: XRD diffraction patterns of cement pastes containing different content of NF fired at 300 ^{o}C; CH = 1; $C\bar{C}$ = 2; C-S-H = 3; β-C_2S = 4; C_3S = 5; Ettringite = 6

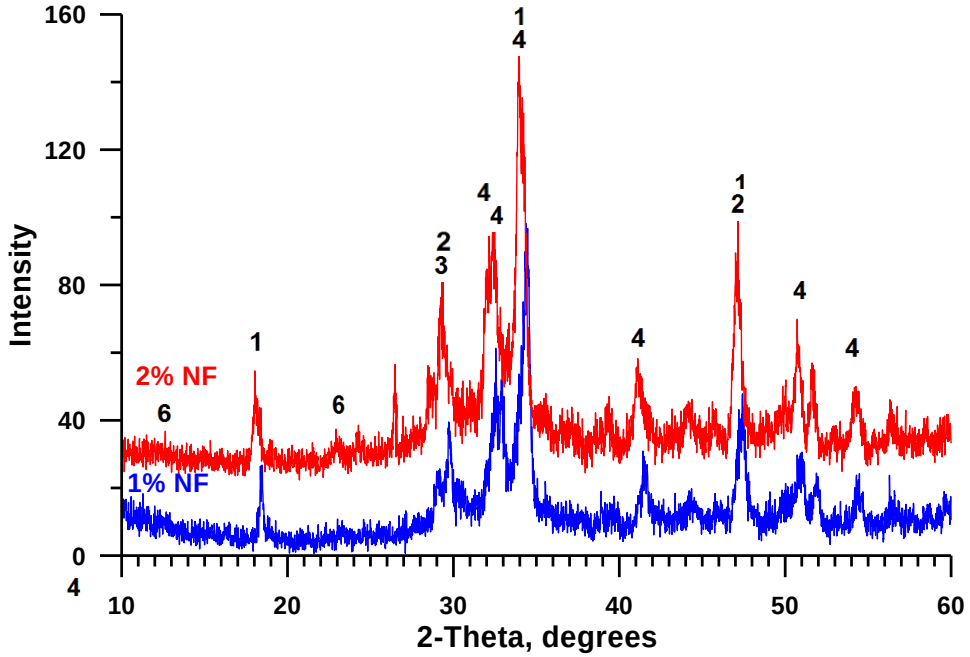

Figure 10: XRD diffraction patterns of cement pastes containing different content of NF fired at 500 ^{o}C; CH = 1; $C\bar{C}$ = 2; C-S-H = 3; β-C_2S = 4; C_3S = 5; Ettringite = 6

4.4.2. Differential Thermal analysis (DTA/TGA):

Figure 11 illustrates DTA/TGA thermograms of mixes I, II and III containing 0, 1, and 2% of NF nano-particles. DTA/TGA thermograms show four main endothermic peaks. The first peak located at 100-125°C, corresponding to the decomposition of C-S-H and C-A-H

hydrated products. The second endothermic peak located at 476-525°C, which is attributed to the dehydroxylation of CH. The third and fourth peaks were observed at 705 and 752°C, due to the decomposition of amorphous and crystalline calcium carbonate [20]. The weight losses at 900°C were found to be 20.48, 18.29 and 20.51% corresponding to mixes I, II and III respectively.

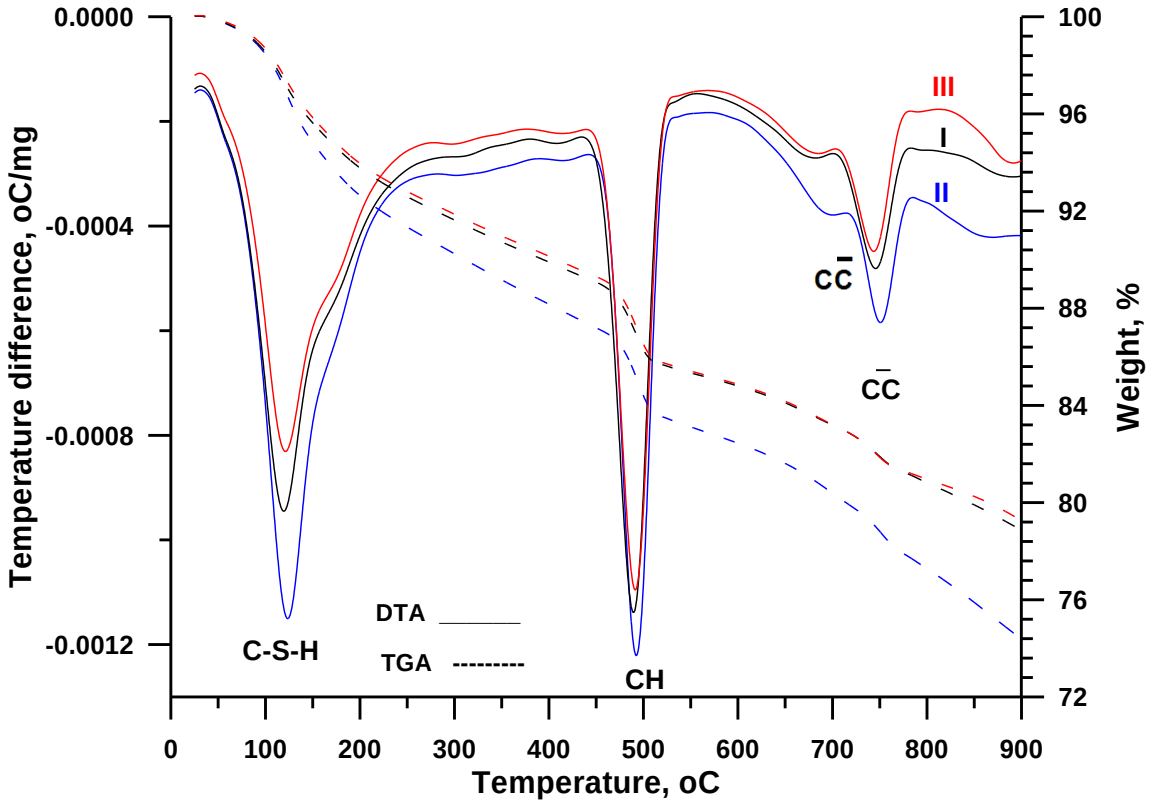

Figure 11: DTA/TGA thermogram of cement pastes containing 0, 1 and 2 mass% NF fired at 300 ^{o}C

The main features of the thermograms are characterized by an increase in the peak area of C-S-H with curing time due to continuous hydration of the cement pastes. The losses of endothermic peak below 200°C were 6.069, 7.379 and 6.079% respectively, which corresponding to the decomposition of C-S-H and C-A-H hydrated products. It is clear that the areas and intensities of the peak characteristic for C-S-H and C-A-H hydrated products increase with NF nano-particles up to 1% as shown in Figure 11.

Figure 12 illustrates DTA/TGA thermograms of mixes IV and VI containing 1 and 2% of NF nano-particles. The weight losses at 900°C were found to be 20.01 and 19.29 % corresponding to mixes IV and VI respectively. The main features of the thermograms are characterized by an increase in the peak area of the decomposition of C-S-H. The losses of endothermic peak below 200°C were 5.63 and 5.79% respectively. It is clear that the areas and

intensities of the peak characteristic for C-S-H and C-A-H hydrated products increase with NF nano-particles up to 2%.

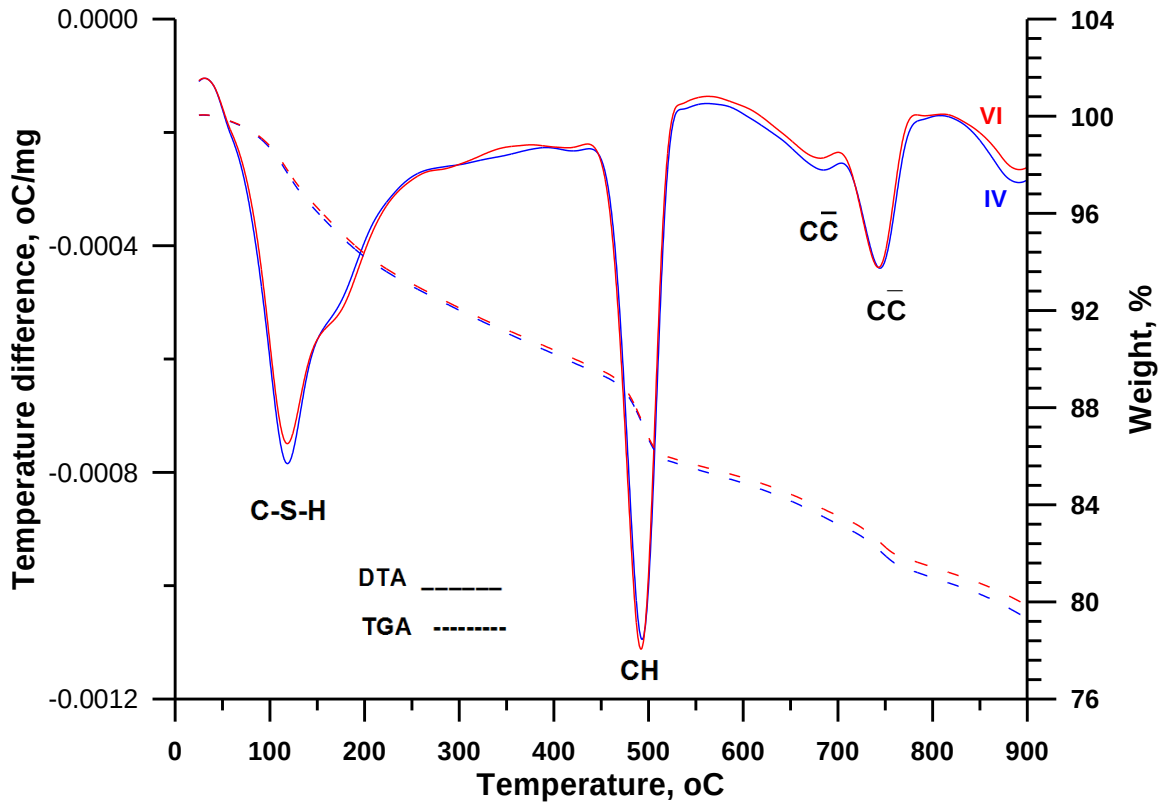

Figure 12: DTA/TGA thermogram of cement pastes containing 1 and 2% NF fired at 500 ^{o}C

3.3. Microstructure:

Scanning electron microscopic studies the microstructure of hardened cement pastes in the presence and absence of NF nanoparticles as shown in Figure 13. Figure 13,A shows a mixture of hydration products having a flocculent and porous structure of ill-crystalline C-S-H and sheets of massive $Ca(OH)_2$ embedded through regions of C-S-H gel. SEM shows also, the paste has a wider pores are available for crystallization of the formed hydrates. NF nano-particles acts as nucleating agent filling the pores as well as accelerating the hydration products to form interlocking dense and compact fibrous C-S-H gel (Figure 13,B). NF nano-particles can improve the filler effect and also the high pozzolanic action of fine particles increases substantially the quantity of C-F-H gel with the cubic and octahedral crystalline in shape. NF nano-particles improve the microstructure in the interfacial transition zones [14]. NF nano-particles recover the particle packing density, directing to a reduced volume of larger pores in the cement paste. However, the value of compressive strength in the specimens is not high and better reinforcements such as needle-type nano-particles are resulted. The increase the content of NF nanoparticles (2 mass%), the SEM micrograph shows an amorphous microcrystalline C-

S-H structure with dense spread of small CH crystals with the presence of micro-crack (Figure 13,C).

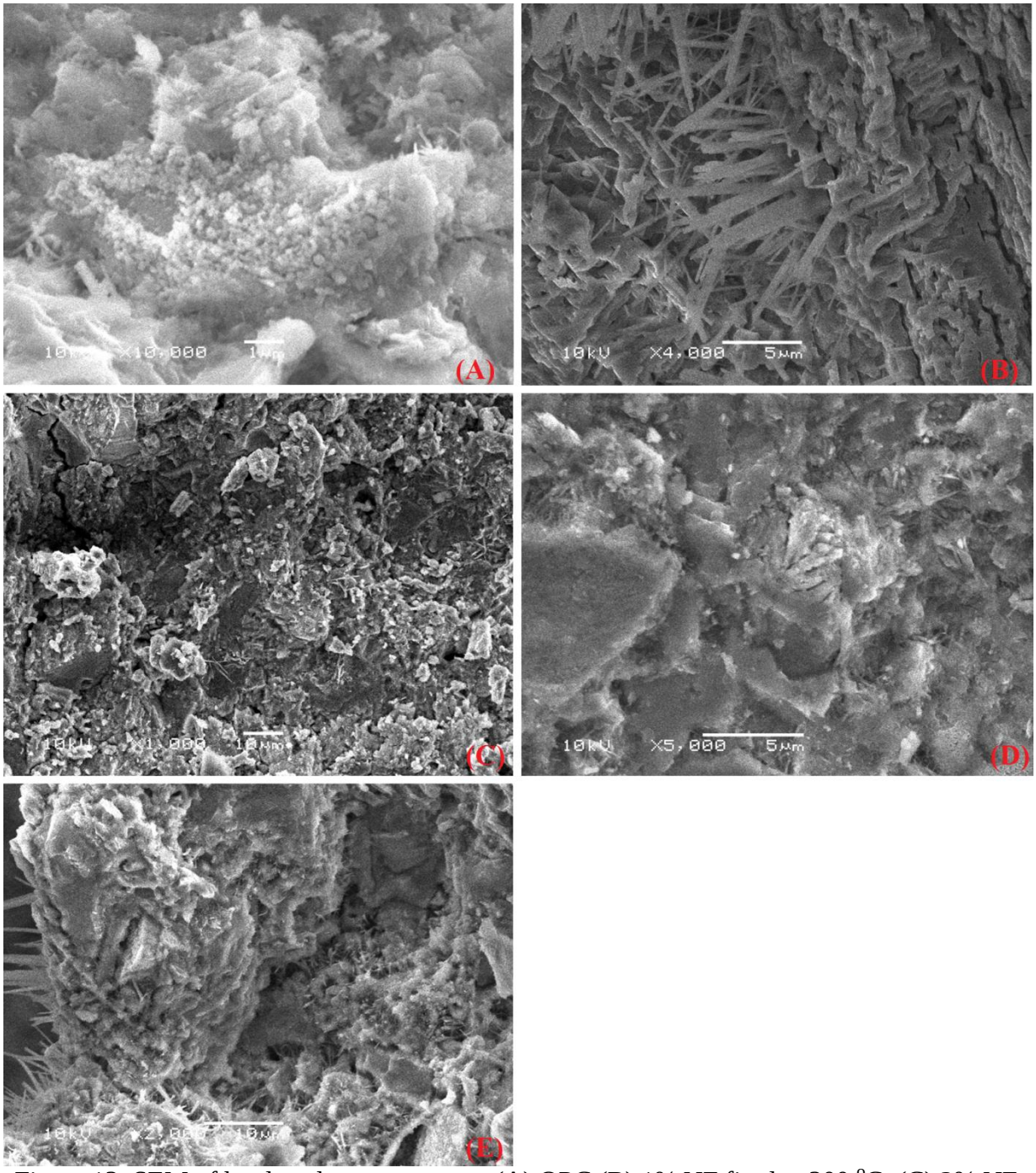

Figure 13: SEM of hardened cement pastes; (A) OPC (B) 1% NF fired at 300 ^{o}C; (C) 2% NF fired at 300 ^{o}C; (D) 1% NF fired at 500 ^{o}C; (E) 2% NF fired at 500 ^{o}C

SEM micrograph as shown in Figure 13,D, shows the presence of less crystalline character of CH which appeared as small hexagonal crystals as well as the presence of amorphous and C-S-H gel like with lower degrees of crystallinity. The increase the content of NF nano-particles (2 mass%, mix VI), the micrograph displays a mixture of hydration products having C-S-H gel in large quantity responsible for bridging cement particles and producing a

rigid closed system. The paste has a higher compressive strength than paste containing 1mass% NF nano-particles as well as neat OPC paste (Figure 13,E).

4. Conclusions:

1. The results show that the presence of NF nano-particles compressive strength show a higher value compare to pastes without NF nano-particles. It is found that the cement could be advantageously replaced with NF nano-particles up to 2.0% fired at 300^{o}C or/and 500^{o}C.
2. The values of chemically combined water content increases with the NF content up to 1mass%. Increase of the content of NF nano-particles up to 2%, the chemically combined water content decreases, but still higher than that of the neat OPC paste.
3. The results show that the free lime content of OPC paste increases, whereas the free lime contents of cement pastes containing NF nano-particles decrease due to the formation of C—F—H gel.
4. NF nano-particles accelerating the hydration products to form interlocking dense and compact fibrous C-S-H gel. The increase the content of NF nanoparticles (2 mass%), the SEM micrograph shows an amorphous microcrystalline C-S-H structure with dense spread of small CH crystals with the presence of micro-crack.

References:

1. Joshi, R. C.; Thomas, O.J. Utilization of modified fly ash. Report. *University of Calgary, Canada.* **1991**, 36.
2. Mehta, P. K. Pozzolanic and cementitious by-products as mineral admixtures for concrete. *Am. Concr. Institute. Publ.* **1979**, 1182.
3. Mitchell, D.R.G.; Hinczak, I.; Day, R.A. Interaction of silica fume with calcium hydroxide solusions and hydration cement pastes. *Cem. Concr. Res*, **1998**, *28*, 1571-1584.
4. Zhu, W.; Bartos, P.J.M.; Porro, A. Application of nanotechnology in construction, summary of a state-of-the-art report. *Mater. Struct*. **2004**,*37*, 649–658.
5. Sobolev, K. Flores, I.; Roman Hermosillo, R.; Leticia, M.; Martınez, T. *Nanomaterials and nanotechnology for high performance cement composites*. Proceedings of ACI

Session on ‘‘*Nanotechnology of Concrete*: *Recent Developments and Future Perspectives*’’ November 7, **2006**; Denver, USA.

6. Rashad, A.M. A synopsis about the effect of nano-Al_2O_3, nano Fe_2O_3, nano-Fe_3O_4 and nano-clay on some properties of cementitious materials – a short guide for civil engineer, *Mater. Des.* **2013**,*52*, 143–157.
7. Gaitero, J.J.; Campillo, I.; Mondal, P.; Shah, S.P. Small changes can make a great difference. *Transport. Res. Rec.: J. Transport. Res. Board* **2010**; 2141,1–5.
8. Torgal, F.P.; Jalali, S. *Eco-efficient Construction and Building Materials*, Springer-Verlag London Limited, **2011**.
9. Bartos, P.J.M. *Nanotechnology in construction: a roadmap for development*, in: Z. Bittnar, P.J.M. Bartos, J. Nemecek, V. Smilauer, J. Zeman (Eds.), *Nanotechnology in Construction*: Proceedings of the NICOM3 (3rd International Symposium on Nanotechnology In Construction), Czech Republic, Prague, **2009**, pp. 15–26.
10. Amer, A.A.; Abdullah, N.I. Behavior of Portland Cement Pastes Admixed With Nano-Iron Oxide at Elevated Temperature. *Inter. J. Eng. Res. & Techno.* **2014**,*3;(9),* 1473-1487.
11. Amer, A.A.; El-Sokkary, T.M.; Abdullah, N.I. Thermal durability of OPC pastes admixed with nano iron oxide. *HBRC J***.** (Accepted for publication 2015).
12. Sobolev, K.; Ferrada-Gutiérrez, M. How nanotechnology can change the concrete", American. *Ceramic. Society. Bulletin*. **2005,** *10*, 14-17.
13. Nazari, A. Assessment of the effects of Fe_2O_3 nanoparticles on water permeability, workability, and setting time of concrete. *J. Comp. Mater.* **2011**, *45,* (8), 923-930
14. Ali Khoshakhlagh, Ali Nazari,Gholamreza Khalaj, Effects of Fe_2O_3 Nanoparticles on Water Permeability and Strength Assessments of High Strength Self-Compacting Concrete, *J. Mate. Sci. & Techno*. **2012**, *28, (1),* 73–82.
15. El-Tawil A.A. The effect of carbothermic reduction on energy consumption of iron blast-furnace. M. Sc. Menoufiya University, 2012.
16. *ASTM Designation*: C-150, 2007.
17. Heikal, M.; Ali, A.; Ismail, M.N.; Awad, S.; Ibrahim, N.S. 'Behavior of composite cement pastes containing silica nano-particles at elevated temperature. *Constr. Buil. Mater.* **2014**, 70, 339-350.
18. Hewlett P.C. *Lea's Chemistry of Cement and Concrete,* 4th Ed., Edward Arnold, London, **2004**.

19. Abd-El-Eziz, M.A.; Heikal, M. Hydration characteristics and durability of cements containing fly ash and limestone subjected to Qaron's Lake Water. *Adv. Cem. Res.* **2009**, *21*, 91-99.
20. Frias, M.; Cabrera, J. Influence of MK on the reaction kinetics in MK/lime and MK-blended cement systems at 20°C. *Cem. Concr. Res*. **2001**,*31*,519–527.